

# PCCP

Accepted Manuscript



This is an *Accepted Manuscript*, which has been through the Royal Society of Chemistry peer review process and has been accepted for publication.

*Accepted Manuscripts* are published online shortly after acceptance, before technical editing, formatting and proof reading. Using this free service, authors can make their results available to the community, in citable form, before we publish the edited article. We will replace this *Accepted Manuscript* with the edited and formatted *Advance Article* as soon as it is available.

You can find more information about *Accepted Manuscripts* in the [Information for Authors](#).

Please note that technical editing may introduce minor changes to the text and/or graphics, which may alter content. The journal's standard [Terms & Conditions](#) and the [Ethical guidelines](#) still apply. In no event shall the Royal Society of Chemistry be held responsible for any errors or omissions in this *Accepted Manuscript* or any consequences arising from the use of any information it contains.



## ARTICLE

## Metastable Charge-Transfer State of Californium(III) Compounds

Guokui Liu,<sup>a,\*</sup> Samantha K. Cary,<sup>b</sup> Thomas E. Albrecht-Schmitt<sup>b</sup>

Received 00th January 20xx,  
Accepted 00th January 20xx

DOI: 10.1039/x0xx00000x

www.rsc.org/

Among a series of anomalous physical and chemical properties of Cf(III) compounds revealed by recent investigations,<sup>1,2</sup> the present work addresses the characteristics of the optical spectra of An(HDPA)<sub>3</sub>·H<sub>2</sub>O (An = Am, Cm, and Cf), especially the broadband photoluminescence from Cf(HDPA)<sub>3</sub>·H<sub>2</sub>O induced by ligand-to-metal charge transfer (CT). As a result of strong ion-ligand interactions and the relative ease of reducing Cf(III) to Cf(II), a CT transition occurs at low energy (< 3 eV) via the formation of a metastable Cf(II) state. It is shown that the systematic trend in CT transitions of the lanthanide series is not paralleled by actinide elements lighter than Cf(III), and californium represents a turning point in the periodicity of the actinide series. Analyses and modeling of the temperature-dependent luminescence dynamics indicate that the metastable Cf(II) charge-transfer state undergoes radiative and non-radiative relaxations. Broadening of the CT transition arises from strong vibronic coupling and hole-charge interactions in the valence band. The non-radiative relaxation of the metastable CT state results from a competition between phonon-relaxation and thermal tunneling that populates the excited states of Cf(III).

### Introduction

The 5*f* actinides prior to americium can be stabilized in multiple oxidation states in both coordination complexes and materials with extended structures. Beyond plutonium, oxidation states beyond 3+ are difficult to attain because the 5*f* orbitals are quite low in energy and are somewhat contracted. This localizes the valence electrons and renders them rather unreactive.<sup>1, 3</sup> Hence, the barriers for the oxidation or reduction of americium, curium, and berkelium roughly parallel that of lanthanides, and formal oxidation states other than 3+ are difficult to achieve. However, starting at californium, and continuing through nobelium, a steady decrease in the standard reduction potentials occurs that indicates that the divalent oxidation state is becoming increasingly thermodynamically stable.<sup>4, 5</sup> In fact, the most stable oxidation state of nobelium is 2+. While the unreactive nature of No(II) might be attributed to its closed-shell, 5*f*<sup>14</sup> configuration, Yb(II), which is also *f*<sup>14</sup>, spontaneously oxidizes in protic media.<sup>6, 7</sup> Hence, other factors are clearly at play in late actinides that are not present in lanthanides.

Prior to californium, divalent actinides are highly reactive and much less stable than their lanthanide counterparts. This is exemplified by Am(II), which can be stabilized by doping into

<sup>a</sup> Chemical Sciences and Engineering Division, Argonne National Laboratory, Argonne, Illinois 60439

<sup>b</sup> Department of Chemistry and Biochemistry, Florida State University, Tallahassee, Florida 32306

\* gkliu@anl.gov

host lattices such as  $\text{CaF}_2$ ,<sup>8</sup> but is in general much more reactive than  $\text{Eu(II)}$ , its lanthanide analog, and few  $\text{Am(II)}$  compounds are known to exist.<sup>9</sup> Ostensibly there is nothing special about the  $5f^{10}$  configuration, and yet  $\text{Cf(II)}$  compounds, such as  $\text{CfX}_2$  ( $X = \text{Cl, Br, I}$ ) can be prepared by stoichiometric reactions of californium metal with halogens.<sup>10,11</sup> Coexistence of the 3+ and 2+ oxidation states of californium or other heavier actinides in same compound has not been reported. The standard reduction potential for the  $\text{Cf(III)/Cf(II)}$  couple is -1.6 eV, close to that of the  $\text{Sm(III)/Sm(II)}$  couple.<sup>12</sup> One expects that the CT energy of  $\text{Cf(III)}$  would depend on the ligand complexes in a similar way as that of the lanthanides.<sup>13,14</sup> In complexes where redox reactions are inactive, CT transitions would enable the measurement of the reduction potentials and  $5f$  energy levels relative to the valence band. Both of these would assist in probing bond attributes as well.

For trivalent lanthanides in complexes and compounds, the CT transition, which converts a lanthanide ion from 3+ to 2+ and leaves a hole ( $h^+$ ) in the valence band, is a common phenomenon widely observed in optical spectra. In many inorganic compounds, the charge-transfer energies of  $\text{Sm}^{3+}$ ,  $\text{Eu}^{3+}$ , and  $\text{Yb}^{3+}$  are typically less than 4 eV, falling into the visible region. The charge-transfer energy varies between different lanthanide ions, but the difference is independent of the type of compound. An empirical model was established to position the energy levels for each divalent lanthanide relative to valence and conduction band states.<sup>13</sup> In the reverse process of CT, charge-hole recombination releases the CT energy and relaxation occurs. In the  $4f$  series, radiative CT luminescence has been observed mostly from  $\text{Yb}$ -compounds, whereas in other systems, non-radiative relaxation populates the low-lying  $4f^n$  states. There is another type of CT that converts 3+ to 2+ ions in compounds such as  $\text{CaF}_2$ . A trivalent lanthanide ion replacing  $\text{Ca}^{2+}$  is stabilized with charge compensation. In this case, CT transitions often create a metastable or long-lived divalent lanthanide ion.<sup>15</sup>

CT transitions are commonly observed in actinyl complexes, especially in uranyl compounds in which CT absorption in blue and UV region leads to intense luminescence in the visible region.<sup>16,17</sup> The energy of uranyl CT is not strongly dependent on complexation because it involves predominantly a  $\text{U(VI)}$  center and the two terminal oxide anions. Based on molecular orbital theory, CT in uranyl is described as an electronic transition between molecular orbitals  $3\sigma$  and  $5f_{\delta\phi}$ .<sup>18</sup> Although the  $5f^n$  energy levels of the trivalent actinides have similar structures as that of the  $4f^n$  configurations, little is known about the systematic behavior of CT of the trivalent actinides. Liu and Jensen<sup>19</sup> found that in the absorption spectrum of  $\text{Am}(\text{Et}_2\text{dtc})_3(\text{bipy})$ ,  $\text{Am(III)}$  to  $\text{Am(II)}$  CT occurs above  $22000 \text{ cm}^{-1}$ , which is close to the value for  $\text{Am(III)}$  in  $\text{An(HDPA)}_3\cdot\text{H}_2\text{O}$  ( $\text{DPA} = 2,6\text{-pyridinedicarboxylate}$ ) observed in the present work. Nugent et al. reported the energy of CT transition in  $\text{CfBr}_3$  at  $35,700 \text{ cm}^{-1}$ . However, for  $\text{Cf(III)}$  in  $\text{Cf(HDPA)}_3\cdot\text{H}_2\text{O}$  studied in the present work, the ligand-to- $\text{Cf(III)}$  CT energy is reduced to below  $20000 \text{ cm}^{-1}$ . For comparison, the standard reduction potential of the  $\text{Cf}^{3+}\text{-Cf}^{2+}$  couple is -1.6 eV ( $\sim 13000 \text{ cm}^{-1}$ ).<sup>4,20</sup>

## Results and discussion

### a. Spectra of 5f-5f transitions and L-An(III) CT transitions

The experimental procedures for synthesis and characterization of the  $\text{An(HDPA)}_3\cdot\text{H}_2\text{O}$  compounds were described in a previous report by Cary et al.<sup>2</sup> In the spectra shown in Fig. 1, two types of bands with quite different characteristics are apparent. Relatively narrower bands in the absorption spectra of  $\text{An(HDPA)}_3\cdot\text{H}_2\text{O}$  ( $\text{An} = \text{Am, Cf}$ ) are given arising from the electronic transitions of trivalent actinide ions within the  $5f^n$  configurations,  $n=6, 9$  for  $\text{Am(III)}$  and  $\text{Cf(III)}$  respectively. Similar results were obtained from  $\text{CfB}_6\text{O}_8(\text{OH})_5$ .<sup>1</sup> The energy levels measured from these band centers are systematically in good agreement with that of the trivalent actinide ions in other crystalline compounds such as  $\text{LaCl}_3$  in which the  $5f$  states are localized and with spectroscopic

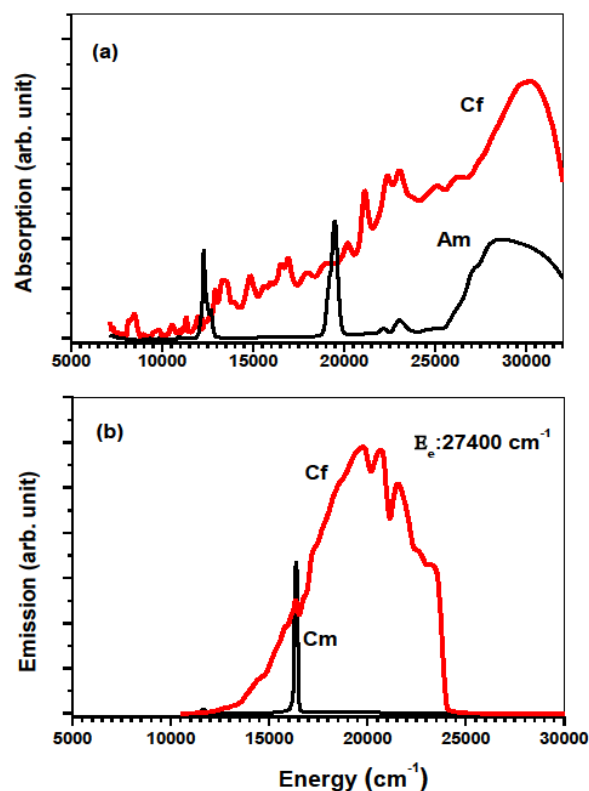


Fig. 1. (a) Absorption spectra of  $\text{Cf(HDPA)}_3\cdot\text{H}_2\text{O}$  and  $\text{Am(HDPA)}_3\cdot\text{H}_2\text{O}$ . (b) luminescence spectra of  $\text{Cf(HDPA)}_3\cdot\text{H}_2\text{O}$  excited at  $27400 \text{ cm}^{-1}$ . The high energy side of the luminescence spectra was cut off by the instrument. The sharp peak at  $16375 \text{ cm}^{-1}$  in the luminescence spectra is from  $^{245}\text{Cm(III)}$  in the sample of  $\text{Cf(HDPA)}_3\cdot\text{H}_2\text{O}$ . The luminescence spectrum of  $^{248}\text{Cm(HDPA)}_3\cdot\text{H}_2\text{O}$  is plotted in (b) for comparison. It only has one sharp peak for the  $5f^7(^6P_{7/2} \rightarrow ^8S_{7/2})$  transition without vibronic broadening.

properties similar to that of the  $4f$  states.<sup>21</sup> As elucidated in Fig. 2, the centers of the narrower absorption bands shown in Fig. 1(a) match the calculated energies of the corresponding SLJ multiplets. Therefore, this result suggests that the  $5f^1$  states of Am(III) and Cf(III) in the DPA compounds have the properties that follow a general trend of trivalent actinide ions in complexes and compounds.<sup>22</sup> Significantly intense and broad bands are also apparent in the absorption spectra. In Am(HDPA)<sub>3</sub>·H<sub>2</sub>O, the broadband starts from 26000 cm<sup>-1</sup>, and in Cf(HDPA)<sub>3</sub>·H<sub>2</sub>O, broadband absorption starts from much lower energy level approximately at 15000 cm<sup>-1</sup>. Based on the energy levels plotted in Fig. 2, it is obvious that the broadband absorption in the high energy (short wavelength) region and emission band from Cf(HDPA)<sub>3</sub>·H<sub>2</sub>O cannot be attributed to  $5f$ - $5f$  transitions. Instead, charge-transfer transition is the origin of the broadband absorption and emission. In Cf(HDPA)<sub>3</sub>·H<sub>2</sub>O, Cf(III) is coordinated with six oxygen atoms with bond length varying from 2.363 Å to 2.476 Å,<sup>2</sup> whereas the bond length between Cf(III) and three nitrogen in the pyridine rings is longer than 2.5 Å. The CT transitions would occur from the  $2p$  orbitals of both O and N to the Cf- $5f$  orbitals, but more favorably from O- $2p$  because ligand-to-metal charge transfer is strongly dependent on the metal-ligand distance. However, in reality CT is a redistribution of charge density between the Cf(III) ion and its surrounding ligands. Unless a sophisticated quantum calculation is accomplished, currently, we do not have precise information to determine quantitatively the CT origins.

As shown in Fig. 1 (b), the photoluminescence observed in Cf(HDPA)<sub>3</sub>·H<sub>2</sub>O does not have the characteristics of  $5f$ - $5f$  transitions but charge-transfer and vibronic transitions. A similar luminescence spectrum was also observed in CfB<sub>6</sub>O<sub>8</sub>(OH)<sub>5</sub>.<sup>1</sup> First, the energy levels of Cf(III) do not permit the luminescence that stretches from 14000 cm<sup>-1</sup> up to 24000 cm<sup>-1</sup>. It is noticed in Fig. 1(b) that the high energy side of the

luminescence spectra was cut off by the instrument. Depending on the excitation energy, the actual high-energy end of the luminescence band can be much higher than 24000 cm<sup>-1</sup>. According to energy gap law,<sup>23, 24</sup> and based on the energy levels structures shown in Fig. 2, if the luminescence is from an excited state of Cf(III), the highest luminescence energy should be less than 20000 cm<sup>-1</sup> from the lowest crystal-field level of  $J=5/2$  multiplet dominated by a free-ion state of <sup>5</sup>P<sub>5/2</sub>. In fact, except for the red luminescence from the  $J=7/2$  state of a minor Cm(III) impurity at 16375 cm<sup>-1</sup>, no other  $5f$ - $5f$  luminescence could be detected from the Am(III) and Cf(III) compounds. For the Am-compound, the excited state <sup>5</sup>D<sub>1</sub> has a much larger energy gap separated from the low-lying <sup>5</sup>D<sub>0</sub> and <sup>7</sup>F<sub>6</sub> states, but no luminescence was observed. It is understood that non-radiative, phonon relaxation and concentration quenching prevent radiative relaxation from the excited states of Am<sup>3+</sup> and Cf<sup>3+</sup>. Second, like the Cm<sup>3+</sup> luminescence band, luminescence originating from  $5f$ - $5f$  transitions should have bandwidth comparable to that of the  $5f$  absorption bands. With all the experimental information, the observed broadband luminescence from the Cf compound does not arise from  $5f$ - $5f$  transitions as previously believed.<sup>1</sup>

As shown in Fig. 1 (b) and previously reported,<sup>2</sup> the Cm(HDPA)<sub>3</sub>·H<sub>2</sub>O compound produced a single, sharp luminescence line at 611 nm (16361 cm<sup>-1</sup>) as shown in Fig. 1(b), where vibronic coupling is absent. It is plotted for comparison with the Cf luminescence spectrum shown in the same figure in which a sharp peak from Cm(III) exists also in the spectrum of Cf(HDPA)<sub>3</sub>·H<sub>2</sub>O as the results of  $\alpha$ -decay of <sup>249</sup>Cf to <sup>245</sup>Cm. Here the orange self-luminescence at 16161 cm<sup>-1</sup> is exactly the same as that found by external excitation of long-lived <sup>248</sup>Cm(III) compounds where the photoluminescence is clearly  $5f$  in origin.<sup>25</sup> Accordingly, the broadband in the Am(III) absorption spectrum (Fig. 1(a)) can also be assigned to CT transition. This assignment is in agreement with that the CT energy of the Am compound is higher than that of the Cf compound. It should be pointed out that such a change in CT energy contradicts the systematic trend of CT variation in the  $4f$  series.<sup>13, 14</sup> The CT energy of Eu(III), the analog of Am(III), is always lower than that of Dy(III), the analog of Cf(III), and all others in the  $4f$  series.

Based on the above analysis and previous studies on Cf oxidation states, the broadband luminescence and absorption in the Cf-compound are attributed to the ligand-to-metal CT transitions that reduce Cf(III) to Cf(II). As a result of this CT transition, a photon is emitted when the hole recombines with Cf(II) back to Cf(III) in a radiative relaxation process. In fact, for heavier actinides, the divalent oxidation state is stable with respect to oxidation. Divalent actinide compounds such as CfCl<sub>2</sub> and EsCl<sub>2</sub> were successfully synthesized but no such complexes of divalent heavy lanthanides could be stabilized. In the previous studies, Cary et al revealed a significant reduction of ion-ligand bond distances in the trivalent actinide series. An average Am–O, Cm–O, and Cf–O bond distances, as well as the An–N distances were found to decrease approximately 0.05 Å from Am(III) to Cf(III).<sup>2</sup> This suggests increase of covalent effects across the actinide series.<sup>26</sup> With regard to lowering of the energy levels and increasing of 2+

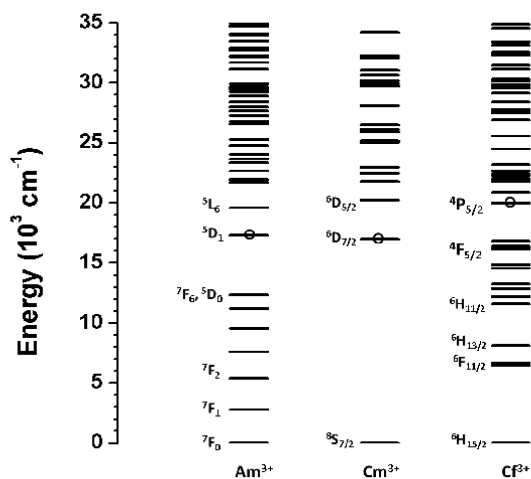


Fig. 2. Partial energy levels of free-ion states of Am<sup>3+</sup>, Cm<sup>3+</sup> and Cf<sup>3+</sup> calculated using energy parameters obtained for An<sup>3+</sup> in LaCl<sub>3</sub>. For ions in compounds, the circles mark the most likely emitting states in the visible region.

stability to facilitate CT in the visible region of wavelength, Cf(III) might be a second turning point after Am(III) in the series. However, if all of these perturbations are simply the result of the metastability of Cf(II), then samarium would display these same properties because its standard reduction from Sm(III) to Sm(II) occurs at the same potential as that of californium.<sup>27</sup> However, samarium does not display these features. In californium, additional factors are clearly at play, the most important of which are the involvement of 5*f*, 6*d*, 7*s*, and 7*p* orbitals in bonding. Because of the covalence which depends on ligands, the series trend determined by free-ion properties is not expected to be followed as well as that of the lanthanides.<sup>13</sup>

The broadband absorption and luminescence in the Cf(HDPA)<sub>3</sub>·H<sub>2</sub>O compound are interpreted as CT transitions that convert Cf(III) to Cf(II) with a hole created in the valence band of the compound. The bandwidth of CT transition, absorption and emission, is significantly broader than that of the 5*f*-5*f* transitions. As shown schematically in Fig. 3, we assume that the ground state energy level of Cf(III),  $E_g(\text{Cf}^{3+})$ , is

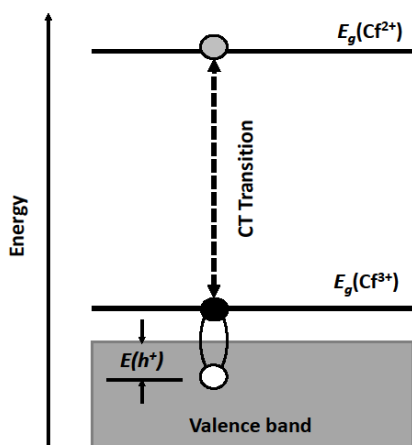


Fig. 3. Energy level schemes of the divalent and trivalent Cf ions relative to the valence band of the compound. It is assumed that the ground state of Cf(III) is above the valence band and charge-transfer transitions can occur from the top and inside of the valence band with hole energy  $E(h^+)$  below the band top.

above the valence band, and the CT transitions can occur from the top as well as inside the valence band. Energetically, this assumption explains the broad bandwidth and the shift of the luminescence spectrum as a function of excitation energy shown in Fig. 1.

A CT transition creates a hole ( $h^+$ ) in the valence band that can be several eV's wide. As a result, the energy of CT transition depends on the location of the hole inside the valence band. If CT starts from the top of the valence band, and ends in the ground state of the divalent actinide ion, CT energy is a measure of the location of the ground state of the divalent actinide relative to the top of the valence band. Otherwise, as

elucidated in Fig. 2, CT energy is larger for transitions initiated inside the valence band. Therefore, for a *f*-element ion in compounds,

$$E^{CT}(3+) = E_{Vf}(2+) + E(h^+), \quad (1)$$

where  $E_{Vf}(2+)$  is the energy of the divalent ion above the valence band with lattice relaxation energy  $E_{rel}$  included, and  $E(h^+)$  is the energy of the hole underneath the valence band. Eq. (1) explains partially the profile of the CT absorption and luminescence. Measured at the low energy edges of the broadband absorption in the spectra of Am(HDPA)<sub>3</sub>·H<sub>2</sub>O and Cf(HDPA)<sub>3</sub>·H<sub>2</sub>O shown in Fig. 1, the CT energy is approximately 28000 cm<sup>-1</sup> (~ 3.5 eV) and 15000 cm<sup>-1</sup> (~ 1.9 eV), respectively, for Am(III) and Cf(III). Not observed in the present work, the CT energy for the Cm(III) compound is expected to be much higher than that of the Am(III) compound.

### b. Dynamics of CT luminescence

Depending on the dynamics of ion-ligand interactions, there are several mechanisms that also contribute to the spectrum broadening. First, after charge transfer, trivalent Cf(III) becomes Cf(II) with a larger ionic radius. A strong lattice relaxation leads to a large offset in the configuration

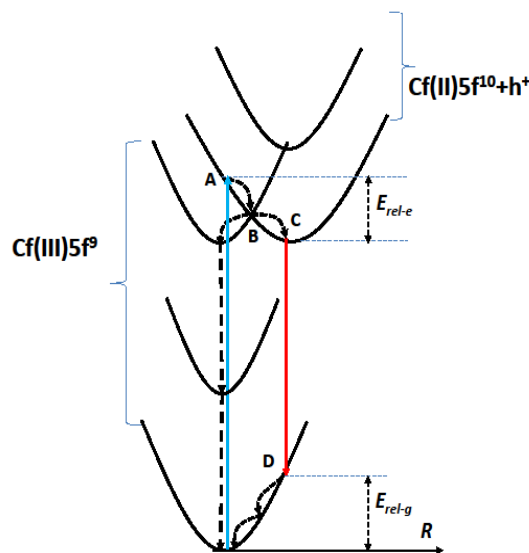


Fig. 4. Configuration coordinate, energy potentials, and relaxation channels of CT vibronic transitions in Cf(III) compounds. The CT excitation ends at point A of the Cf(II) ground state potential then relaxes to B and C via non-radiative lattice relaxation and to D via radiative relaxation. The shift of the Cf(II) potential along *R* indicates a CT-induced bond expansion.

coordinate diagram as shown in Fig. 4. For lanthanide CT, this accounts for up to 0.5 to 1 eV in CT bandwidth.<sup>13</sup> Secondly, CT transitions end in more than one electronic state. In absorption, the excited CT states involve the crystal-field splitting of the  $5f^{10}$  multiplets of Cf(II), and the profile of the CT emission band depends on the low-energy states of the  $5f^9$  configuration (primarily  ${}^6H_{15/2}$ ) and the top states (HOMO) of the ligand complex. Other contributions to the observed CT bandwidth may include ion-site distortion and crystalline defects, which should be small and insignificant in single-site crystalline compounds.

Based on Franck-Condon principle for vibronic transitions and assuming that the CT emission spectrum is a superposition of vibronic transitions involving multiple vibrational modes ( $\nu_i$ ), and electronic states ( $E_k$ ),<sup>16, 28</sup> the expected spectral profile of the CT vibronic transitions would include multi-phonon progressions and frequency mixing in terms of  $Mh\nu_i + Nh\nu_j$ . If the distribution of the lattice vibrational oscillators is of Gaussian shape, the intensity function of the vibronic transitions to electronic state  $k$  is of the following form.<sup>29</sup>

$$f_{MN}(E_k, \nu_i, \nu_j) = \frac{S_i^M S_j^N}{M! N! \sqrt{2\pi(M\sigma_i^2 + N\sigma_j^2)}} \exp\left[-\frac{[E - (E_k + Mh\nu_i + Nh\nu_j)]^2}{2(M\sigma_i^2 + N\sigma_j^2)}\right], \quad (2)$$

with values of  $M$  and  $N$  increase from 0, 1, 2, ... to high orders of phonon states. Eq. (2) describes the intensity changes as a function of  $M$  and  $N$ .  $S_i$  and  $S_j$  are vibronic coupling strength, known as Huang-Rhys parameter for vibrational mode  $\nu_i$  and  $\nu_j$ , respectively.

Eq. (2) was used for simulating the CT emission spectrum of Cf(II) in comparison with the experimental spectrum of Cf(HDPA)<sub>3</sub>·H<sub>2</sub>O. As shown in Fig. 5, the simulated spectrum has

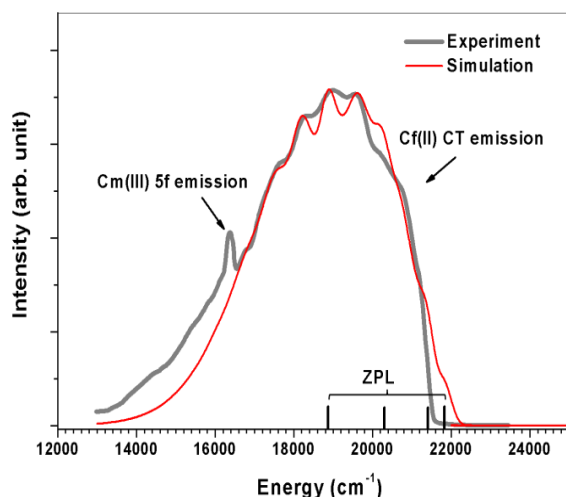


Fig. 5. Comparison of CT luminescence of Cf(HDPA)<sub>3</sub>·H<sub>2</sub>O recorded at 420 nm (23810 cm<sup>-1</sup>) excitation with simulated spectrum. The four vertical lines mark the ZPLs resulting from the simulation. The 5f-5f emission band from Cm(III) in the sample was excluded from the simulation.

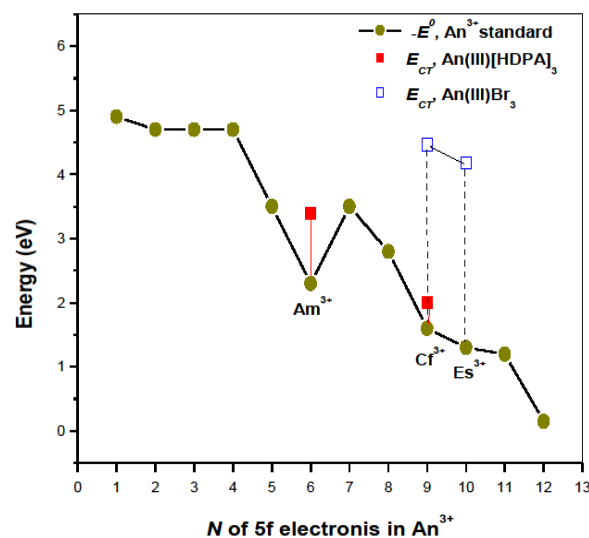


Fig. 6 Comparison of charge transfer energies of An(III) in An(HDPA)<sub>3</sub>·H<sub>2</sub>O and AnBr<sub>3</sub> with the standard reduction potentials ( $-E^0$ ) of trivalent actinide ions.

the major features in good agreement with the experimental one. Three vibrational frequencies were resulted from the simulation. These vibrational frequencies,  $\nu_1 = 590$  cm<sup>-1</sup>,  $\nu_2 = 655$  cm<sup>-1</sup> and  $\nu_3 = 698$  cm<sup>-1</sup> are expected to be the frequencies of the Cf-ligand stretching modes. Also obtained from the simulation, the value of  $S = 1.1$  is close to that for uranyl CT transitions, and a large value of  $\sigma = 180$  cm<sup>-1</sup> reflects the intrinsic width of the Gaussian distribution and the influence of the low-frequency modes not included in the simulation.<sup>28</sup> The simulation resulted in four electronic energy levels of the ground state marked in Fig. 5 as zero-phonon-lines (ZPLs). To be further verified by theoretical calculations of the CT states, the splitting of the CT ground state up to 3000 cm<sup>-1</sup> is an indication of strong ion-ligand covalence.

The standard reduction potential  $E^0$  for the Cf<sup>3+</sup> and Cf<sup>2+</sup> ion couple is about -1.6 eV (see Fig. 6),<sup>4</sup> which is lower than that of the Am<sup>3+</sup> - Am<sup>2+</sup> couple and approximately the same as that for the Sm<sup>3+</sup> - Sm<sup>2+</sup> couple in the 4f-series.<sup>27</sup> For the 4f-series, CT energies between different ion couples are correlated and the differences in CT energies for different ion couples are independent of ligands.<sup>13</sup> There is no sufficient information on whether such a correlation is preserved or not between the CT energies for actinides in different complexes and compounds in which the reduction potential varies significantly. It should be preserved if the influence of ion-ligand covalence is insignificant and variation of CT energies depends primarily on the ligand field. Although the electronic properties are different from that of their lanthanide analogues, Cf(III) and its neighbors in the heavy actinides series may preserve such a systematic trend. A previous work by Nugent et al. measured the CT energy of CfBr<sub>3</sub> and EsBr<sub>3</sub>.<sup>27</sup> As shown in Fig. 6, the difference in the CT energies between Cf(III) and Es(III) is

identical as that for the standard reduction potential. In the present case, a significantly strong crystal-field in  $\text{An}(\text{HDP A})_3$  pushes down the ground state energy level of  $\text{Am}(\text{II})$  and  $\text{Cf}(\text{II})$  toward the valence band. The CT energy of  $\text{Cf}(\text{III})$  is much smaller than that in  $\text{CfBr}_3$ . With regard to the systematic trend, the variation of the CT energy from  $\text{Am}(\text{HDP A})_3\text{-H}_2\text{O}$  to  $\text{Cf}(\text{HDP A})_3\text{-H}_2\text{O}$  is quite different from that in the standard reduction potentials. Therefore, the comparison made with limited information from the two pairs of actinide ions indicates that the lighter elements before Cf and the heavier ones from Cf in the actinide series have different properties in terms of CT and reduction of oxidation states.

In reverse CT, combination of the transferred charge and hole may lead to both radiative and non-radiative relaxation. The absence of luminescence from the  $\text{Am}(\text{III})$  compound indicates that the CT state near  $28000\text{ cm}^{-1}$  and the most probable emitting state of  $5f^6 ({}^5D_1)$  near  $18000\text{ cm}^{-1}$  are quenched via non-radiative phonon relaxation. However, in the  $\text{Cf}(\text{III})$  compound, CT luminescence with a lifetime longer than  $1\text{ }\mu\text{s}$  was observed at room temperature and become much stronger below  $150\text{ K}$ , indicating that the  $\text{Cf}(\text{III})$  CT state is much more stable than that of  $\text{Am}(\text{III})$  in the same compound. In fact, this is for the first time that CT luminescence from divalent actinide ion in a compound is detected. The relaxation mechanisms and channels are elucidated in Fig. 4. The temperature dependent photoluminescence indicates the competition of the radiative and non-radiative relaxation processes. It is apparent that as shown in Fig. 1 (b) and Fig. 5, under the excitation with different photon energies of  $23810$  and  $27400\text{ cm}^{-1}$ , respectively, the luminescence spectrum is invariant in the low energy side but stretches up as a function of excitation energy in the high energy side. Generally known as Stokes shift, the luminescence spectrum is a convolution of vibronic broadening in the  $\text{Cf}(\text{III})$  and  $\text{Cf}(\text{II})$  electronic states and variation of the hole energy in the valence band. From the absorption spectrum and the luminescence spectrum, we can estimate that the overall bandwidth for the Cf charge-transfer vibronic transition is broader than  $15000\text{ cm}^{-1}$  ( $\sim 2\text{ eV}$ ) with contribution from hole-energy distribution as well as lattice relaxation and vibronic coupling.

The decay of CT luminescence is quite non-exponential on the time scales from  $300\text{ ns}$  to  $6\text{ }\mu\text{s}$ ,<sup>2</sup> an indication of variation in the lifetime of the excited CT state for CT transition initiated in different levels of the valence band. In other words, the variation of the luminescence decay time is primarily due to the different time scales of hole-charge recombination. In the CT state, multi-phonon relaxation is also an important process that influences the excited state lifetime and the luminescence intensity. In phonon-relaxation, the integrated luminescence intensity as a function of temperature is expected to obey the energy gap law,<sup>23,24</sup>

$$I_{MP}(T) = I_0 \left[ 1 - \exp\left(-\frac{h\nu}{kT}\right) \right]^p, \quad (3)$$

where  $h\nu$  is the energy of the phonons involved in the relaxation process. A more rigorous approach would account for an ensemble of phonons with different energies, symmetries, and population densities, but  $h\nu$  is often approximated to have a single value. The value of  $p = \Delta E/h\nu$  is the number of phonons involved in the decay process to bridge the energy gap  $\Delta E$  between the emitting state and the next lower energy state.

In addition to multi-phonon relaxation, excitation quenching through tunneling or thermalization from the emitting state must be taken into account in the form of Arrhenius equation. In the present case as shown in Fig. 4, relaxation from the ground state  $\text{Cf}(\text{II})$  into the excited states of  $\text{Cf}(\text{III})$  across the configuration potential (point B in Fig. 4) would be the leading process of luminescence quenching. Taking into account of both multi-phonon relaxation and tunneling, the intensity of the CT luminescence as a function of temperature is modified into<sup>30-33</sup>

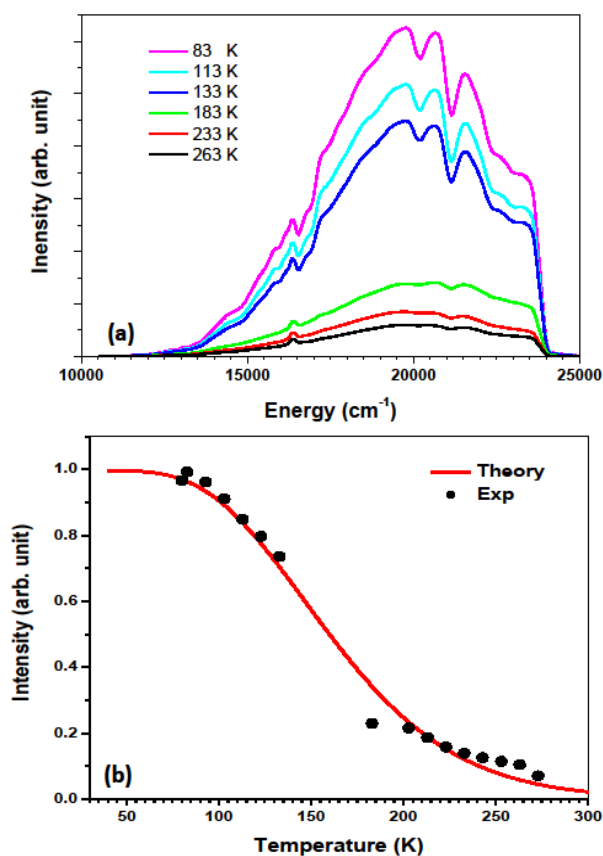


Fig. 7. Temperature dependence of Cf luminescence for  $\text{Cf}(\text{HDP A})_3\text{-H}_2\text{O}$  recorded at  $365\text{ nm}$  excitation. The data plotted in (b) are peak intensities of the luminescence spectra, and the curve is a fitting with Eq. (3).

$$I_{CT}(T) = I_0 \left[ 1 + \alpha \exp\left(-\frac{E_a}{kT}\right) \right]^{-1} \left[ 1 - \exp\left(-\frac{h\nu}{kT}\right) \right]^p, \quad (4)$$

where  $E_a$  is the energy barrier that separates between the potential of Cf(III) and Cf(II) and  $\alpha$  is a parameter to be determined in fitting experimental data. Eq. (4) was applied to fitting the temperature dependence of the peak intensity of the CT luminescence. The values of the fitting parameters are:  $h\nu = 500 \text{ cm}^{-1}$ ,  $E_a = 320 \text{ cm}^{-1}$ ,  $\alpha = 7$  and  $p = 30$ . As shown in Fig.7, the dynamics of the CT luminescence is satisfactorily described by the theoretical model of multi-phonon relaxation plus excited-state quench. It confirms that both relaxation mechanisms contribute competitively to the Cf(II)  $\rightarrow$  Cf(III) relaxation.

## Conclusions

Analyses of the optical spectra and luminescence dynamics confirmed a ligand-to-metal charge-transfer transition of Cf(III) in DPA and borate compounds. Optical excitation in the visible region is able to reduce Cf(III) to Cf(II) in those compounds. The photoluminescence emitted from the CT state further indicates that a Cf(II)-hole pair is metastable and the subsequent recombination occurs via radiative and non-radiative relaxation channels. Significant vibronic broadening in the absorption and emission spectra indicates changes in both electronic configuration and coordination structure. The low-lying Cf(III) states do not completely quench the CT state. Such a metastable CT state is unusual as far as the  $f$ -element paradigm of electronic properties is concerned. Increasing ion-ligand interactions are the driving force that push down the energy level of CT state toward the valence band, thus helping stabilizing the divalent oxidation state. Largely because of the stabilization of the divalent oxidation state, a second transition in the periodicity of the actinide series occurs at Cf(III) as the turning point. The systematic trend of CT observed in the lanthanide series is unlikely followed in the actinide series lighter than Cf(III). Additional factors are clearly at play, the most important of which is the actinide orbital hybridization that mixes  $5f$ ,  $6d$ ,  $7s$ , and  $7p$  orbitals in bonding with oxygen ligands. Therefore, CT energies including the splittings of the ground CT state are expected to depend on the degrees of these orbital mixtures. Further studies are required for quantitatively determining the influence of orbital hybridization and ion-ligand covalence.

## Acknowledgements

This work was funded by the Division of Chemical Sciences, Geosciences, and Biosciences, Office of Basic Energy Sciences of the U.S. Department of Energy under contract DE-AC02-06CH11357 (GL) and DE-FG02-13ER16414 (SKC and TEA).

## Notes and references

1. M. J. Polinski, E. B. Garner, R. Maurice, N. Planas, J. T. Stritzinger, T. G. Parker, J. N. Cross, T. D. Green, E. V. Alekseev, S. M. Van Cleve, W. Depmeier, L. Gagliardi, M. Shatruk, K. L. Knappenberger, G. K. Liu, S. Skanthakumar, L. Soderholm, D. A. Dixon and T. E. Albrecht-Schmitt, *Nat Chem*, 2014, **6**, 387-392.
2. S. K. Cary, M. Vasiliu, R. E. Baumbach, J. T. Stritzinger, T. D. Green, K. Diefenbach, J. N. Cross, K. L. Knappenberger, G. Liu, M. A. Silver, A. E. DePrince, M. J. Polinski, S. M. V. Cleve, J. H. House, N. Kikugawa, A. Gallagher, A. A. Arico, D. A. Dixon and T. E. Albrecht-Schmitt, *Nat Commun*, 2015, DOI: 10.1038/ncomms7827.
3. M. L. Neidig, D. L. Clark and R. L. Martin, *Coord. Chem. Rev.*, 2013, **257**, 394-406.
4. N. M. Edelstein, J. Fuger, J. J. Katz and L. R. Morss, in *The Chemistry of the Actinide and Transactinide Elements*, eds. L. R. Morss, N. M. Edelstein and J. Fuger, Springer, Netherlands, 2006, vol. 3, p. 1779.
5. R. J. M. Konings, L. R. Morss and J. Fuger, in *The Chemistry of the Actinide and Transactinide Elements* eds. L. R. Morss, N. M. Edelstein and J. Fuger, Springer, The Netherlands, 2006, vol. 4, pp. 2113-2224.
6. D. C. Hoffman, R. A. Henderson, K. E. Gregorich, D. A. Bennett, R. M. Chasteler, C. M. Gannett, H. L. Hall, D. M. Lee, M. J. Nurmia, S. Cai, R. Agarwal, A. W. Charlop, Y. Y. Chu, G. T. Seaborg and R. J. Silva, *J Radioan Nucl Ch Ar*, 1988, **124**, 135-144.
7. U. W. Scherer, J. V. Kratz, M. Schädel, W. Bröchle, K. E. Gregorich, R. A. Henderson, D. Lee, M. Nurmia and D. C. Hoffman, *Inorganica Chimica Acta* 1988, **146**, 249-254.
8. N. Edelstein, W. Easley and R. McLaughlin, *J Chem Phys*, 1966, **44**, 3130-3131.
9. W. H. Runde and W. W. Schulz, in *The Chemistry of the Actinide and Transactinide Elements*, eds. L. R. Morss, N. M. Edelstein and J. Fuger, Springer, The Netherlands, 2006, vol. 2, pp. 1265-1395.
10. J. P. Young, K. L. Vander Sluis, G. K. Werner, J. R. Peterson and M. Noe, *J. Inorg. Nuclear Chem.*, 1975, **37**, 2497-2501.
11. J. R. Peterson, R. L. Fellows, J. P. Young and R. G. Haire, *Radiochem. Radionol. Letters*, 1977, **31**, 277-282.
12. N. M. Edelstein, J. Fuger, J. J. Katz and L. R. Morss, in *The Chemistry of the Actinide and Transactinide Elements*, eds. L. R. Morss, N. M. Edelstein and J. Fuger, Springer Netherlands, 2006, vol. 3, pp. 1753-1835.
13. P. Dorenbos, *J. Phys.: Condens. Matter*, 2003, **15**, 8417-8434.
14. G. Liu, M. P. Jensen and P. M. Almond, *J. Phys. Chem. A*, 2006, **110**, 2081-2088.
15. B. Jassemnejad and S. W. S. McKeever, *J. Phys. D: Appl. Phys.*, 1987, **20**, 323-328.
16. G. Liu, N. P. Deifel, C. L. Cahill, V. V. Zhurov and A. A. Pinkerton, *J Phys Chem A*, 2012, **116**, 855-864.
17. R. G. Denning, in *Structure and Bonding*, ed. M. J. Clarke, Springer, Berlin, 1992, vol. 79, pp. 215-276.
18. S. Matsika and R. M. Pitzer, *J. Chem. Phys.*, 2001, **105**, 637-645.
19. G. Liu and M. Jensen, *Unpublished*
20. L. J. Nugent, R. D. Baybarz and J. L. Burnett, *The Journal of Physical Chemistry*, 1969, **73**, 1177-1178.

## ARTICLE

PCCP

21. W. T. Carnall, *J. Chem. Phys.*, 1992, **96**, 8713-8726.
22. G. Liu and J. V. Beitz, in *The Chemistry of the Actinide and Transactinide Elements*, eds. L. R. Morss, J. Fuger and N. M. Edelstein, Springer, Berlin, 2006, pp. 2013-2111.
23. L. A. Riseberg and H. W. Moos, *Phys Rev Lett*, 1967, **25**, 1423-1426.
24. L. A. Riseberg and H. W. Moos, *Phys. Rev.*, 1968, **174**, 429-438.
25. G. Liu, J. V. Beitz and J. Huang, *J. Chem. Phys.*, 1993, **99**, 3304-3311.
26. M. B. Jones and A. J. Gaunt, *Chem Rev*, 2013, **113**, 1137-1198.
27. L. J. Nugent, R. D. Baybarz, J. L. Burnett and J. L. Ryan, *J. Phys. Chem.*, 1973, **77**, 1528-1539.
28. G. Liu, *J Lumin*, 2014, **152**, 7-10.
29. M. Wagner, *J Chem Phys*, 1964, **41**, 3939-3943.
30. D. Y. Zhai, L. X. Ning, Y. C. Huang and G. Liu, *J Phys Chem C*, 2014, **118**, 16051-16059.
31. M. Raukas, S. A. Basun, W. vanSchaik, W. M. Yen and U. Happek, *Appl Phys Lett*, 1996, **69**, 3300-3302.
32. M. Godlewski, *J Alloy Compd*, 1995, **225**, 41-44.
33. E. Mihokova, V. Jary, M. Fasoli, A. Lauria, F. Moretti, M. Nikl and A. Vedda, *Chem Phys Lett*, 2013, **556**, 89-93.